A QCQP Approach for OPF in Multiphase Radial Networks with Wye and Delta Connections

Ahmed S. Zamzam*, Changhong Zhao†, Emiliano Dall'Anese†, and Nicholas D. Sidiropoulos*
* Department of Electrical and Computer Engineering, University of Minnesota, Minneapolis, MN 55455
† National Renewable Energy Laboratory, Golden, CO 80401

***Abstract*—This paper examines the AC Optimal Power Flow (OPF) problem for multiphase distribution networks featuring renewable energy resources (RESs). We start by outlining a power flow model for radial multiphase systems that accommodates wye-connected and delta-connected RESs and non-controllable energy assets. We then formalize an AC OPF problem that accounts for both types of connections. Similar to various AC OPF renditions, the resultant problem is a nonconvex quadratically-constrained quadratic program. However, the so-called Feasible Point Pursuit - Successive Convex Approximation algorithm is leveraged to obtain a feasible and locally-optimal solution. The merits of the proposed solution approach are demonstrated using two unbalanced multiphase distribution feeders with both wye and delta connections.**

I. Introduction

The AC optimal power flow (OPF) problem aims at optimizing the operation of a power system based on specified performance and operational objectives, while abiding to physical constraints and engineering limits [1], [2]. The cost function can capture a variety of performance objectives, including (but not limited to) the minimization of power losses over the network, generation cost from traditional fossil-fuel units [3], and power curtailment from renewable sources of energy [4]. Maximization of customer benefits from ancillary-service provisioning [5], [6] is also considered in a number of OPF formulations for distribution systems [4], [7]–[9]. The AC OPF problem has been the fundamental problem in power systems since it was introduced in 1962 [1]. Unfortunately, the nonlinearity of the AC power-flow equations renders the OPF problem nonconvex and NP-hard in its general form [3], [10].

This paper focuses on unbalanced multiphase distribution networks with renewable energy resources (RESs). A power flow model for radial multiphase systems that accommodates wye-connected and delta-connected distributed energy resources is first outlined. Then, an AC OPF problem that accounts for both types of connections as well as pertinent operational constraints (e.g., voltage constraints) is outlined. The problem formulation is further manipulated in order to restate the AC OPF in an equivalent nonconvex quadratically-constrained quadratic program (QCQP) form. With this reformulation in place, the proposed solution methodology leverages the so-called Feasible Point Pursuit Successive Convex Approximation (FPP-SCA) algorithm for nonconvex QCQPs [11]. The FPP-SCA replaces the nonconvex constraints by inner convex surrogates around a specific point to construct a convex restriction of the original problem. Such restriction may lead to infeasibility, even if the original problem is feasible. A key principle behind FPP-SCA is to allow a controllable amount of constraint violations to enable the algorithm to make progress towards feasibility in its initial stages. In this paper, FPP-SCA is empirically shown to be very effective in solving the AC OPF for radial multiphase systems with both wye and delta connections, and with a variety of operational objectives. The proposed approach considerably broadens our previous contribution [12] by considering systems with both wye and delta connections.

Several approaches have been previously used to handle OPF problems for distribution networks [13]–[18]. For example, in [13], a convex relaxation approach was used to handle the problem based on the well-known semidefinite relaxation. However, the model used accounts only for balanced wye-connected loads. Further, feasible solutions may be found only under certain problem formulations [16]. As a generalization of semidefinite relaxation, moment relaxation methods [19], [20] were proposed, where moments of higher orders were also considered using the Lassarre Hierarchy. Although shown to be tighter than semidefinite relaxation, there is no known upper limit on the moment order required to approach the optimal solution, and the problem becomes practically intractable for large scale networks or a relatively high moment order.

Relative to prior works, the methodology proposed here can handle both wye and delta connections, and it inherits the merits of [12] in providing an effective way to identify a feasible and locally-optimal solution for a variety of objective functions for the RESs in the OPF formulation.

This paper is organized as follows. The network model is outlined in Section II and the QCQP formulation of the AC OPF problem is presented in Section III. Then, the FPP-SCA-based algorithm is described in Section IV. Section V provides numerical results and Section VI concludes the paper.

The work of A.S. Zamzam and N.D. Sidiropoulos was partially supported by NSF under grant CIF-1525194. The work of C. Zhao and E. Dall'Anese was supported by the U.S. Department of Energy under Contract No. DE-AC36-08GO28308 with the National Renewable Energy Laboratory; funding provided by the Advanced Research Projects Agency-Energy (ARPA-E) under the Network Optimized Distributed Energy Systems (NODES) program. The U.S. Government retains and the publisher, by accepting the article for publication, acknowledges that the U.S. Government retains a nonexclusive, paid-up, irrevocable, worldwide license to publish or reproduce the published form of this work, or allow others to do so, for U.S. Government purposes.

II. Multiphase Radial Network Model

Notation. Let $\mathbb{R}$, $\mathbb{C}$, and $\mathbb{N}$ denote the set of real, complex, and (positive) natural numbers, respectively. For $n \in \mathbb{N}$, let $\mathbb{H}^{n\times n}$ denote the space of all n-by-n Hermitian matrices. For a scalar, vector, or matrix A, let A^T, A^*, and A^H denote its transpose, element-wise conjugate, and conjugate transpose, respectively. For an index set S, let A_S denote the set $\{A_s \mid s \in S\}$, where the subscript S is omitted when its meaning is clear from the context.

A. Power flow model

Consider a radial multiphase distribution network with nodes collected in the set $\mathcal{N} = \{0, 1, \ldots, n\}$. Let 0 represent the substation or the point of common coupling, and define $\mathcal{N}^+ := \mathcal{N} \setminus \{0\}$. Let $\mathcal{E}$ denote the set of lines connecting the buses. In particular, each line connects an ordered pair (l, m) of buses, where bus l lies between bus 0 and bus m. We use $(l, m) \in \mathcal{E}$ and $l \to m$ interchangeably, and denote $l \sim m$ if either $l \to m$ or $m \to l$. In addition, let $\mathcal{R} \subseteq \mathcal{N}^+$ represent a set that collects the buses with RESs.

For simplicity of notation and exposition, assume that all the buses $k \in \mathcal{N}$ and lines $(l, m) \in \mathcal{E}$ have three phases a, b, c, and define the sets $\Phi := \{a, b, c\}$ and $\Phi_\Delta := \{ab, bc, ca\}$. However, the proposed approach can be straightforwardly applied to distribution networks that feature a mix of three-phase, two-phase, and single-phase nodes. Let v_n^ϕ denote the complex voltage phasor at bus $k \in \mathcal{N}$ and $\phi \in \Phi$, and let $\mathbf{v}_k$ be a column vector that collects the complex voltages at all the phases for node k, i.e., $\mathbf{v}_k := [v_k^a,\ v_k^b,\ v_k^c]$. Similarly, let the vector $\mathbf{I}_{lm}$ collect the complex current that flows in the line $(l, m) \in \mathcal{E}$ for all phases in Φ. Let $y_k \in \mathbb{C}^{3\times 3}$ denote the shunt admittance at bus k, and denote as $z_{lm} \in \mathbb{C}^{3\times 3}$ the series impedance of line $l \sim m$.

Without loss of generality, assume that every bus $k \in \mathcal{N}$ has three wye-connected net loads (one on each phase, with grounded neutral) and three delta-connected net loads (one across each pair of phases, ungrounded). Define the complex vector $\mathbf{s}_{\mathrm{Y},k}^{(L)} \in \mathbb{C}^3$ to be a vector that collects the wye-connected loads at bus $k \in \mathcal{N}$ for all phases. In a similar way, define $\mathbf{s}_{\Delta,k}^{(L)} \in \mathbb{C}^3$ to be a complex column vector that collects the delta-connected loads at bus $k \in \mathcal{N}$. Notice that both wye and delta connection may be present at the same node of the network model when different distribution transformers with either delta and/or wye primary connections are bundled together for network reduction purposes (e.g., when two transformers are connected through a short low-impedance distribution line). Based on prevailing ambient conditions, let the maximum available active powers for the wye-connected RESs at phases $\phi \in \Phi$ of node $k \in \mathcal{R}$ be collected in a column vector $\overline{\mathbf{p}}_{\mathrm{Y},k}^{(R)} \in \mathbb{R}^3$. Also, let the apparent powers injected by these RESs be collected in a vector $\mathbf{s}_{\mathrm{Y},k}^{(R)} = \mathbf{p}_{\mathrm{Y},k}^{(R)} + i\mathbf{q}_{\mathrm{Y},k}^{(R)}$. Similarly, let $\overline{\mathbf{p}}_{\Delta,k}^{(R)} \in \mathbb{R}^3$ and $\mathbf{s}_{\Delta,k}^{(R)} \in \mathbb{C}^3$ be the corresponding vectors for the delta-connected sources at bus k. Let $\mathbf{s}_{\mathrm{Y},k} := [s_{\mathrm{Y},k}^a, s_{\mathrm{Y},k}^b, s_{\mathrm{Y},k}^c]^T = \mathbf{s}_{\mathrm{Y},k}^{(L)} - \mathbf{s}_{\mathrm{Y},k}^{(R)}$ denote the net wye-connected loads at bus k. Also, let $\mathbf{s}_{\Delta,k} := [s_{\Delta,k}^{ab},\ s_{\Delta,k}^{bc},\ s_{\Delta,k}^{ca}]^T = \mathbf{s}_{\Delta,k}^{(L)} - \mathbf{s}_{\Delta,k}^{(R)}$ and $\mathbf{I}_{\Delta,k} := [I_{\Delta,k}^{ab},\ I_{\Delta,k}^{bc},\ I_{\Delta,k}^{ca}]^T$ denote the power consumptions and currents of delta-connected net loads at bus k, respectively. If neither loads nor (sources) are present at a particular phase for a particular type of connection, then the corresponding element of $\mathbf{s}_{\mathrm{Y},k}^{(L)}$, $\mathbf{s}_{\mathrm{Y},k}^{(R)}$, $\mathbf{s}_{\Delta,k}^{(L)}$, or $\mathbf{s}_{\Delta,k}^{(R)}$ is set to zero.

Voltages and line currents abide by Ohm's Law, which yields:

$$\mathbf{v}_l - \mathbf{v}_m = z_{lm}\mathbf{I}_{lm}, \quad \forall l \to m. \tag{1}$$

In addition, the power flow equations for the delta-connected loads at bus k can be expressed as

$$\mathbf{s}_{\Delta,k} = \begin{bmatrix} (v_k^a - v_k^b)(I_{\Delta,k}^{ab})^* \\ (v_k^b - v_k^c)(I_{\Delta,k}^{bc})^* \\ (v_k^c - v_k^a)(I_{\Delta,k}^{ca})^* \end{bmatrix}, \quad \forall k \in \mathcal{N}. \tag{2}$$

Power balance at bus $k \in \mathcal{N}$ then implies that:

$$\sum_{i:i\to k} \begin{bmatrix} v_k^a (I_{ik}^a)^* \\ v_k^b (I_{ik}^b)^* \\ v_k^c (I_{ik}^c)^* \end{bmatrix} = \sum_{j:k\to j} \begin{bmatrix} v_k^a (I_{kj}^a)^* \\ v_k^b (I_{kj}^b)^* \\ v_k^c (I_{kj}^c)^* \end{bmatrix} + \begin{bmatrix} v_k^a (y_k^a \mathbf{v}_k)^* \\ v_k^b (y_k^b \mathbf{v}_k)^* \\ v_k^c (y_k^c \mathbf{v}_k)^* \end{bmatrix} + \mathbf{s}_{\mathrm{Y},k} + \begin{bmatrix} v_k^a (I_{\Delta,k}^{ab} - I_{\Delta,k}^{ca})^* \\ v_k^b (I_{\Delta,k}^{bc} - I_{\Delta,k}^{ab})^* \\ v_k^c (I_{\Delta,k}^{ca} - I_{\Delta,k}^{bc})^* \end{bmatrix}. \tag{3}$$

Recalling that the network is assumed to have a tree tolopogy, the left-hand-side of (3) represents the power received by bus k from the rest of the network through the distribution line $(i, k) \in \mathcal{E}$. On the other hand, the first term on the right-hand-side represents the power transferred to the network through line $(k, j) \in \mathcal{E}$; the second term accounts for the power drawn to the ground at every phase through the shunt element; the third term represents the apparent power absorbed/generated by the wye-connected loads at the bus; and, the last term represents delta-connected net loads. Notice that the power flow equations (2) and (3) have quadratic terms; using these equations within an optimization task leads to nonconvex problem formulations.

III. QCQP Formulation of Optimal Power Flow

A. Optimal power flow problem

Let p_{loss} denote the active power loss in the network, which is given by

$$p_{loss} = \sum_{\phi\in\Phi} P_0^\phi - \sum_{k\in\mathcal{N}^+} \left(\sum_{\phi\in\Phi} \Re\{s_{\mathrm{Y},k}^\phi\} + \sum_{\phi\in\Phi_\Delta} \Re\{s_{\Delta,k}^\phi\} \right) \tag{4}$$

where P_0^ϕ denotes the active power drawn from the transmission system on phase ϕ at the substation. The second term in (4) represents the net active power consumption at node k. Also, let $\mathbf{p}_{\Delta,k}^{(c)} := \overline{\mathbf{p}}_{\Delta,k}^{(R)} - \mathbf{p}_{\Delta,k}^{(R)} \in \mathbb{R}^3$ denote the active power curtailed at the delta-connected RESs. Similarly, define $\mathbf{p}_{\mathrm{Y},k}^{(c)} := \overline{\mathbf{p}}_{\mathrm{Y},k}^{(R)} - \mathbf{p}_{\mathrm{Y},k}^{(R)} \in \mathbb{R}^3$ as the amount of active power curtailed from the available active power at the wye-connected

RESs at bus k. With these definitions in place, a formulation of the AC OPF problem is given by:

$$\textbf{OPF: } \min \quad C_{loss}(p_{loss}) + \sum_{k\in\mathcal{R}} C_k(\mathbf{p}^{(c)}_{\mathrm{Y},k}, \mathbf{p}^{(c)}_{\Delta,k}) \tag{5a}$$

$$\text{over} \quad \mathbf{s}^{(R)}_{\mathrm{Y},k}, \mathbf{s}^{(R)}_{\Delta,k}, \mathbf{v}_k, \mathbf{I}_{\Delta,k} \in \mathbb{C}^3, \quad \forall k \in \mathcal{N}$$

$$\mathbf{I}_{lm} \in \mathbb{C}^3, \quad \forall l \to m$$

$$\text{s.t.} \quad (1)\text{–}(3)$$

$$\mathbf{s}_{\Delta,k} = \mathbf{s}^{(L)}_{\Delta,k} - \mathbf{s}^{(R)}_{\Delta,k} \quad \forall k \in \mathcal{N} \tag{5b}$$

$$\mathbf{s}_{\mathrm{Y},k} = \mathbf{s}^{(L)}_{\mathrm{Y},k} - \mathbf{s}^{(R)}_{\mathrm{Y},k} \quad \forall k \in \mathcal{N} \tag{5c}$$

$$\mathbf{v}_0 = \mathbf{v}_0^{\text{ref}} \tag{5d}$$

$$\underline{v}^{\phi}_k \le |v^{\phi}_k| \le \overline{v}^{\phi}_k, \quad \forall k \in \mathcal{N}^+, \ \forall \phi \in \Phi \tag{5e}$$

$$\mathbf{p}^{(R)}_{\mathrm{Y},k} \le \overline{\mathbf{p}}^{(R)}_{\mathrm{Y},k} \quad \forall k \in \mathcal{R} \tag{5f}$$

$$\mathbf{p}^{(R)}_{\Delta,k} \le \overline{\mathbf{p}}^{(R)}_{\Delta,k} \quad \forall k \in \mathcal{R} \tag{5g}$$

The power flow equations (1)–(3) impose physical constraints to the OPF. The substation voltage is fixed and given as $\mathbf{v}_0^{\text{ref}}$ in (5d). Constraints on voltage magnitudes at all the other buses are enforced by (5e). Operational constraints on the controllable RESs are enforced by (5f) and (5g). The cost function in (5a) is composed of two terms: the first term is a strongly convex quadratic cost that minimizes the active power loss over the network; and, the second term is a strongly convex function that penalizes the amount of active power curtailed from the RESs. Constraints (5b)–(5c) are imposed on a per-node basis.

B. QCQP reformulation of OPF

To facilitate the application of the FPP-SCA algorithm to the problem at hand, the AC OPF (5) is restated next in an equivalent QCQP form. To this end, define the vector $\mathbf{x}_{lm} := [\mathbf{v}_l^T, \mathbf{I}_{lm}^T]^T$ for all $l \to m$, and $\mathbf{x}_{\Delta,k} := [\mathbf{v}_k^T, \mathbf{I}_{\Delta,k}^T]^T$ for all $k \in \mathcal{N}$. Consider matrices $E_{ij} \in \mathbb{R}^{6\times 6}$ and $\tilde{E}_{ij} \in \mathbb{R}^{3\times 3}$ such that their (i,j)-th element is one (1) and all the other elements are zero (0). Then, (2) can be written as:

$$\mathbf{s}_{\Delta,k} = \begin{bmatrix} \mathbf{x}^H_{\Delta,k}(E_{41} - E_{42})\,\mathbf{x}_{\Delta,k} \\ \mathbf{x}^H_{\Delta,k}(E_{52} - E_{53})\,\mathbf{x}_{\Delta,k} \\ \mathbf{x}^H_{\Delta,k}(E_{63} - E_{61})\,\mathbf{x}_{\Delta,k} \end{bmatrix}, \quad \forall k \in \mathcal{N}. \tag{6}$$

In (3), the term $v^a_k(I^a_{kj})^*$ can be re-written as

$$v^a_k(I^a_{kj})^* = \mathbf{x}^H_{kj} E_{41} \mathbf{x}_{kj}.$$

In a similar way, the product $v^a_k(I^a_{ik})^*$ can be expanded as shown next:

$$\begin{aligned} v^a_k(I^a_{ik})^* &= v^a_i(I^a_{ik})^* - (v^a_i - v^a_k)(I^a_{ik})^* \\ &= v^a_i(I^a_{ik})^* - z^a_{ik}\mathbf{I}_{ik}(I^a_{ik})^* \\ &= \mathbf{x}^H_{ik}\left(E_{41} - z^{aa}_{ik}E_{44} - z^{ab}_{ik}E_{45} - z^{ac}_{ik}E_{46}\right)\mathbf{x}_{ik} \end{aligned}$$

where $z^a_{ik} = [z^{aa}_{ik}, z^{ab}_{ik}, z^{ac}_{ik}]$ is the first row of the impedance matrix z_{ik}. Moreover, we have that

$$V^a_k(y^a_k V_k)^* = \mathbf{v}^H_k \left(y^{aa,*}_k \tilde{E}_{11} + y^{ab,*}_k \tilde{E}_{21} + y^{ac,*}_k \tilde{E}_{31}\right)\mathbf{v}_k.$$

Additionally, for delta connected units, the term $v^a_k(I^{ab}_{\Delta,k} - I^{ca}_{\Delta,k})^*$ can be re-written as

$$v^a_k(I^{ab}_{\Delta,k} - I^{ca}_{\Delta,k})^* = \mathbf{x}^H_{\Delta,k}(E_{41} - E_{61})\,\mathbf{x}_{\Delta,k}.$$

Following similar steps, quadratic expressions of all the other elements in (3) can be obtained and, consequently, (3) can be written as follows:

$$\begin{aligned} &\sum_{i:i\to k} \begin{bmatrix} \mathbf{x}^H_{ik}\left(E_{41} - z^{aa}_{ik}E_{44} - z^{ab}_{ik}E_{45} - z^{ac}_{ik}E_{46}\right)\mathbf{x}_{ki} \\ \mathbf{x}^H_{ik}\left(E_{52} - z^{ba}_{ik}E_{54} - z^{bb}_{ik}E_{55} - z^{bc}_{ik}E_{56}\right)\mathbf{x}_{ki} \\ \mathbf{x}^H_{ik}\left(E_{63} - z^{ca}_{ik}E_{64} - z^{cb}_{ik}E_{65} - z^{cc}_{ik}E_{66}\right)\mathbf{x}_{ki} \end{bmatrix} \\ = &\sum_{j:k\to j} \begin{bmatrix} \mathbf{x}^H_{kj}E_{41}\mathbf{x}_{kj} \\ \mathbf{x}^H_{kj}E_{52}\mathbf{x}_{kj} \\ \mathbf{x}^H_{kj}E_{63}\mathbf{x}_{kj} \end{bmatrix} + \begin{bmatrix} \mathbf{x}^H_{\Delta,k}(E_{41} - E_{61})\,\mathbf{x}_{\Delta,k} \\ \mathbf{x}^H_{\Delta,k}(E_{52} - E_{42})\,\mathbf{x}_{\Delta,k} \\ \mathbf{x}^H_{\Delta,k}(E_{63} - E_{53})\,\mathbf{x}_{\Delta,k} \end{bmatrix} \\ &+\mathbf{s}_{\mathrm{Y},k} + \begin{bmatrix} \mathbf{v}^H_k\left(y^{aa,*}_k\tilde{E}_{11} + y^{ab,*}_k\tilde{E}_{21} + y^{ac,*}_k\tilde{E}_{31}\right)\mathbf{v}_k \\ \mathbf{v}^H_k\left(y^{ba,*}_k\tilde{E}_{12} + y^{bb,*}_k\tilde{E}_{22} + y^{bc,*}_k\tilde{E}_{32}\right)\mathbf{v}_k \\ \mathbf{v}^H_k\left(y^{ca,*}_k\tilde{E}_{13} + y^{cb,*}_k\tilde{E}_{23} + y^{cc,*}_k\tilde{E}_{33}\right)\mathbf{v}_k \end{bmatrix} \end{aligned} \tag{7}$$

for all $k \in \mathcal{N}$, while the voltage magnitude constraints (5e) admit the following equivalent formulation:

$$(\underline{v}^{\phi}_k)^2 \le \mathbf{v}^H_k \tilde{E}_{\phi\phi}\mathbf{v}_k \le (\overline{v}^{\phi}_k)^2, \quad \forall k \in \mathcal{N}^+, \ \forall \phi \in \Phi. \tag{8}$$

Next, let the vector $\mathbf{x}_v \in \mathbb{C}^{3(n+1)}$ collect $\mathbf{v}_k$ for all $k \in \mathcal{N}$. Similarly, let $\mathbf{x}_\Delta \in \mathbb{C}^{3(n+1)}$ be a vector that concatenates $\mathbf{I}_{\Delta,k}$ for all $k \in \mathcal{N}$ and let $\mathbf{x}_i \in \mathbb{C}^{3n}$ stack $\mathbf{I}_{lm}$ for all $(l,m) \in \mathcal{E}$. Define $\tilde{\mathbf{x}}$ as

$$\tilde{\mathbf{x}} = [\mathbf{x}_v^T, \ \mathbf{x}_i^T, \ \mathbf{x}_\Delta^T]^T. \tag{9}$$

and consider the stacked vector of its real and imaginary parts $\mathbf{x} := [\mathrm{Re}(\tilde{\mathbf{x}})^T \ \mathrm{Im}(\tilde{\mathbf{x}})^T]^T$; notice that $\mathbf{x}$ is a rwal vector containing $(18n + 12)$ elements. The quadratic functions (6) and (7) can be written as functions of $\mathbf{x}$. Particularly, (7) involves $6(n+1)$ equations (involving real quantities) while $6(n+1)$ equations are utilized to describe (6)

The OPF problem (5) can then be written as the following QCQP form:

$$\min \quad C_{loss}(p_{loss}) + \sum_{k\in\mathcal{R}} C_k(\mathbf{p}^{(c)}_{\mathrm{Y},k}, \mathbf{p}^{(c)}_{\Delta,k}) \tag{10a}$$

$$\text{over} \quad \mathbf{x}, \{\mathbf{s}^{(R)}_{\mathrm{Y},k}, \mathbf{s}^{(R)}_{\Delta,k}\}_{k\in\mathcal{R}}$$

$$\text{s.t.} \quad \mathbf{A}\mathbf{x} = \mathbf{d} \tag{10b}$$

$$\mathbf{x}^T\mathbf{B}^{\phi}_{\Delta,k}\mathbf{x} = \Re\{s^{\phi}_{\Delta,k}\} \quad \forall \phi \in \Phi_\Delta, \forall k \in \mathcal{N} \tag{10c}$$

$$\mathbf{x}^T\tilde{\mathbf{B}}^{\phi}_{\Delta,k}\mathbf{x} = \Im\{s^{\phi}_{\Delta,k}\} \quad \forall \phi \in \Phi_\Delta, \forall k \in \mathcal{N} \tag{10d}$$

$$\mathbf{x}^T\mathbf{B}^{\phi}_{\mathrm{Y},k}\mathbf{x} = \Re\{s^{\phi}_{\mathrm{Y},k}\} \quad \forall \phi \in \Phi, \forall k \in \mathcal{N} \tag{10e}$$

$$\mathbf{x}^T\tilde{\mathbf{B}}^{\phi}_{\mathrm{Y},k}\mathbf{x} = \Im\{s^{\phi}_{\mathrm{Y},k}\} \quad \forall \phi \in \Phi, \forall k \in \mathcal{N} \tag{10f}$$

$$(\underline{v}^{\phi}_k)^2 \le \mathbf{x}^T\mathbf{M}^{\phi}_k\mathbf{x} \le (\overline{v}^{\phi}_k)^2 \quad \forall \phi \in \Phi, \forall k \in \mathcal{N}^+ \tag{10g}$$

$$\mathbf{s}_{\Delta,k} = \mathbf{s}^{(L)}_{\Delta,k} - \mathbf{s}^{(R)}_{\Delta,k} \quad \forall k \in \mathcal{N} \tag{10h}$$

$$\mathbf{s}_{\mathrm{Y},k} = \mathbf{s}^{(L)}_{\mathrm{Y},k} - \mathbf{s}^{(R)}_{\mathrm{Y},k} \quad \forall k \in \mathcal{N} \tag{10i}$$

$$\mathbf{p}^{(R)}_{\mathrm{Y},k} \le \overline{\mathbf{p}}^{(R)}_{\mathrm{Y},k} \quad \forall k \in \mathcal{R} \tag{10j}$$

$$\mathbf{p}^{(R)}_{\Delta,k} \le \overline{\mathbf{p}}^{(R)}_{\Delta,k} \quad \forall k \in \mathcal{R} \tag{10k}$$

where $\mathbf{B}^{\phi}_{\Delta,k}$, $\tilde{\mathbf{B}}^{\phi}_{\Delta,k}$, $\mathbf{B}^{\phi}_{\mathrm{Y},k}$, and $\tilde{\mathbf{B}}^{\phi}_{\mathrm{Y},k}$ are symmetric matrices that represents the real and imaginary parts of equation (6) and (7), respectively, and their construction is explained in the Appendix. Notice that the values of $\mathbf{s}^{(R)}_{\Delta,k}$ for $k \notin \mathcal{R}$ are set to zero, and hence, they are not considered as optimization variables. The matrix $\mathbf{A}$ and the vector $\mathbf{d}$ are constructed in a way to rewrite the constraints (1) and (5d) in terms of $\mathbf{x}$.

IV. Feasible Point Pursuit Algorithm

A. Feasibility Phase

The FPP algorithm solves a sequence of inner-approximations of the non-convex feasibility set. Since the approximation point is not feasible, the inner-approximations might be empty sets. Therefore, a non-negative common slack variable is added to each approximated constraint in order to ensure feasibility of the iterates, and the slack size is minimized to approach feasibility. Once the slack variable is zero, a feasible point has been found, and the procedure continues to solve a sequence of restricted problems until convergence. In the first phase, the inner-approximations are construted as follows.

We begin with noticing that the constraint (10c) can be written as two inequalities:

$$\mathbf{x}^T\mathbf{B}^{\phi}_{\Delta,k}\mathbf{x} \leq \Re\{s^{\phi}_{\Delta,k}\}, \tag{11a}$$

$$\mathbf{x}^T(-\mathbf{B}^{\phi}_{\Delta,k})\mathbf{x} \leq -\Re\{s^{\phi}_{\Delta,k}\}. \tag{11b}$$

Since the matrix $\mathbf{B}_{kl}$ is indefinite, the constraints (11a)–(11b) are nonconvex. Constraint (11a) can be further re-expressed as

$$\mathbf{x}^T\mathbf{B}^{\phi,(+)}_{\Delta,k}\mathbf{x} + \mathbf{x}^T\mathbf{B}^{\phi,(-)}_{\Delta,k}\mathbf{x} \leq \Re\{s^{\phi}_{\Delta,k}\} \tag{12}$$

where $\mathbf{B}^{\phi,(+)}_{\Delta,k}$ and $\mathbf{B}^{\phi,(-)}_{\Delta,k}$ are the positive semidefinite and the negative semidefinite parts of the matrix $\mathbf{B}^{\phi}_{\Delta,k}$, respectively. For $\mathbf{B}^{\phi,(-)}_{\Delta,k}$, the following inequality holds:

$$(\mathbf{x}-\mathbf{z})^T\mathbf{B}^{\phi,(-)}_{\Delta,k}(\mathbf{x}-\mathbf{z}) \leq 0. \tag{13}$$

Then, expanding the left hand side, the following inequality can be obtained

$$\mathbf{x}^T\mathbf{B}^{\phi,(-)}_{\Delta,k}\mathbf{x} \leq 2\mathbf{z}^T\mathbf{B}^{\phi,(-)}_{\Delta,k}\mathbf{x} - \mathbf{z}^T\mathbf{B}^{\phi,(-)}_{\Delta,k}\mathbf{z}. \tag{14}$$

and a surrogate of the non-convex quadratic constraint (11a) reads

$$\mathbf{x}^T\mathbf{B}^{\phi,(+)}_{\Delta,k}\mathbf{x} + 2\mathbf{z}^T\mathbf{B}^{\phi,(-)}_{\Delta,k}\mathbf{x} \leq \Re\{s^{\phi}_{\Delta,k}\} + \mathbf{z}^T\mathbf{B}^{\phi,(-)}_{\Delta,k}\mathbf{z} + s \tag{15}$$

where the nonnegative slack variable s is added to ensure feasibility. Similarly, (11b) can be replaced by

$$\mathbf{x}^T(-\mathbf{B}^{\phi,(-)}_{\Delta,k})\mathbf{x} - 2\mathbf{z}^T\mathbf{B}^{\phi,(+)}_{\Delta,k}\mathbf{x} \leq -\Re\{s^{\phi}_{\Delta,k}\} - \mathbf{z}^T\mathbf{B}^{\phi,(+)}_{\Delta,k}\mathbf{z} + s. \tag{16}$$

Not unlike (10c), the constraint (10d), (10e), and (10f) are also replaced by similar surrogates. Finally, the lower bound in the constraint (10g) is replaced by the convex restriction

$$2\mathbf{z}^T(-\mathbf{M}^{\phi}_{k})\mathbf{x} \leq -(\underline{v}^{\phi}_{k})^2 + \mathbf{z}^T(-\mathbf{M}^{\phi}_{k})\mathbf{z} + s. \tag{17}$$

Let Ω denote the nonconvex set described by the constraints (10c)–(10g). Similarly, let $\hat{\Omega}(z)$ denote the convex set obtained by replacing the nonconvex constraints (10c)–(10g) with the respective convex surrogates and adding the slack variable s. The optimization problem to be solved at each iteration of the algorithm can be then be formalized as follows:

$$\begin{aligned}
\textbf{OPF-F:}\ \min\quad & s && (18a)\\
\text{over}\quad & s, \mathbf{x}, \{\mathbf{s}^{(R)}_{\mathrm{Y},k}, \mathbf{s}^{(R)}_{\Delta,k}\}_{k\in\mathcal{R}} &\\
\text{s.t.}\quad & \mathbf{A}\mathbf{x} = \mathbf{d} && (18b)\\
& (\mathbf{x}, s) \in \hat{\Omega}(\mathbf{z}_i) && (18c)\\
& \mathbf{s}_{\Delta,k} = \mathbf{s}^{(L)}_{\Delta,k} - \mathbf{s}^{(R)}_{\Delta,k} \quad \forall k \in \mathcal{N} && (18d)\\
& \mathbf{s}_{\mathrm{Y},k} = \mathbf{s}^{(L)}_{\mathrm{Y},k} - \mathbf{s}^{(R)}_{\mathrm{Y},k} \quad \forall k \in \mathcal{N} && (18e)\\
& \mathbf{p}^{(R)}_{\mathrm{Y},k} \leq \overline{\mathbf{p}}^{(R)}_{\mathrm{Y},k} \quad \forall k \in \mathcal{R} && (18f)\\
& \mathbf{p}^{(R)}_{\Delta,k} \leq \overline{\mathbf{p}}^{(R)}_{\Delta,k} \quad \forall k \in \mathcal{R} && (18g)
\end{aligned}$$

The optimization problem (18) can be cast as SOCP which can be solved efficiently in polynomial time. Each problem instance is feasible due to the positive slack variable. This *feasible point pursuit* is tabulated as Algorithm 1.

Initialization: *set* $i = 0$, and choose $\mathbf{z}_0$ to be the flat voltage profile.
repeat
  $\mathbf{x}_i, s \leftarrow$ solution of (18).
  $\mathbf{z}_{i+1} \leftarrow \mathbf{x}_i$.
  $i \leftarrow i + 1$.
until $s < \epsilon_1$ *or* $||\mathbf{x}_i - \mathbf{x}_{i-1}|| \leq \epsilon_1$
Output: $\mathbf{x}_f \leftarrow \mathbf{x}_i$

Algorithm 1: Feasible Point Pursuit Algorithm

B. Refinement Phase

Starting from a feasible point, the nonconvex feasible set is replaced at each iteration by an inner convex approximation. Similar to the feasibility phase, convex surrogates are formulated as convex upper bounds for the nonconvex components of the quadratic constraints. Accordingly, at each iteration, the following problem is solved:

$$\begin{aligned}
\textbf{OPF-R:}\ \min\quad & C_{loss}(p_{loss}) + \sum_{k\in\mathcal{R}} C_k(\mathbf{p}^{(c)}_{\mathrm{Y},k}, \mathbf{p}^{(c)}_{\Delta,k}) && (19a)\\
\text{over}\quad & s = 0, \mathbf{x}, \{\mathbf{s}^{(R)}_{\mathrm{Y},k}, \mathbf{s}^{(R)}_{\Delta,k}\}_{k\in\mathcal{R}} &\\
\text{s.t.}\quad & \mathbf{A}\mathbf{x} = \mathbf{d} && (19b)\\
& (\mathbf{x}, s) \in \hat{\Omega}(\mathbf{z}_i) && (19c)\\
& \mathbf{s}_{\Delta,k} = \mathbf{s}^{(L)}_{\Delta,k} - \mathbf{s}^{(R)}_{\Delta,k} \quad \forall k \in \mathcal{N} && (19d)\\
& \mathbf{s}_{\mathrm{Y},k} = \mathbf{s}^{(L)}_{\mathrm{Y},k} - \mathbf{s}^{(R)}_{\mathrm{Y},k} \quad \forall k \in \mathcal{N} && (19e)\\
& \mathbf{p}^{(R)}_{\mathrm{Y},k} \leq \overline{\mathbf{p}}^{(R)}_{\mathrm{Y},k} \quad \forall k \in \mathcal{R} && (19f)\\
& \mathbf{p}^{(R)}_{\Delta,k} \leq \overline{\mathbf{p}}^{(R)}_{\Delta,k} \quad \forall k \in \mathcal{R} && (19g)
\end{aligned}$$

Note that, since the starting point is feasible, the slack variable s is not required. The sequence generated by the algorithm is always feasible and the sequence of cost functions is non-increasing. Algorithm 2 describes the steps of the refinement phase.

Initialization: *set* $i = 0$, and $\mathbf{z}_0 = \mathbf{x}_f$.
repeat
  $\mathbf{x}_i \leftarrow$ solution of (19).
  $\mathbf{z}_{i+1} \leftarrow \mathbf{x}_i$.
  $i \leftarrow i + 1$.
until $\frac{\mathbf{x}_{i-1} - \mathbf{x}_i}{\mathbf{x}_{i-1}} < \epsilon_2$
Output: $\mathbf{x}_{opt} \leftarrow \mathbf{x}_i$

Algorithm 2: Successive Convex Approximation Algorithm

V. Experimental Results

In this section, the efficacy of the proposed approach is demonstrated using two radial distribution feeders featuring both delta and wye connections. The proposed approach is shown to be able to provide a solution that minimizes the sum of the amount of power curtailed by the RESs and the power losses in the network while respecting the physical constraints.

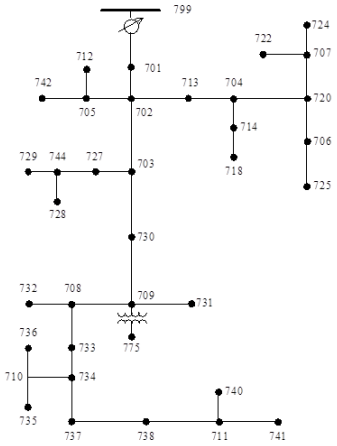

Fig. 1: IEEE 37-node test feeder.

In the first experiment, the IEEE 37-node test feeder shown in Fig. 1 is considered. Since this feeder features only delta-connected loads, wye connections are added as described in Table III. The cost function $C_{loss}(p_{loss})$ is defined to be the square of p_{loss}. Additionally, the cost function $C_k(\mathbf{p}^{(c)}_{\mathrm{Y},k}, \mathbf{p}^{(c)}_{\Delta,k})$ is defined to be the square of the amount of active power curtailed at bus k. The amount of power injected by every renewable source is shown in Table I, along with the amount of power available from the RESs. At the optimal solution using the FPP-SCA algorithm, the total power loss in the network is 58.6 KW, while the total amount of curtailed power at the renewables is 6.54 KW out of the 765.44 KW available active power at the RESs. Fig. 2 shows that the voltage profiles obtained using our proposed algorithm satisfy

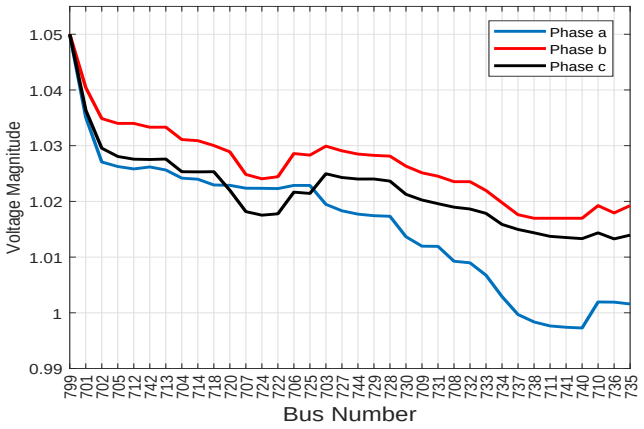

Fig. 2: The optimal voltage profile (in pu) using FPP-SCA for IEEE 37-node test feeder.

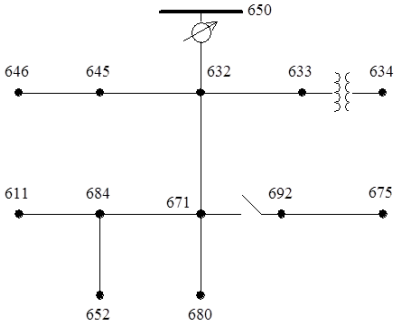

Fig. 3: IEEE 13-node test feeder.

the magnitude constraints; i.e., the obtained operational point is indeed feasible (and optimal).

The IEEE 13-bus distribution network shown in Fig 3 is utilized in the second test. In this network, there are five shunt capacitor banks installed at different nodes that can provide reactive power. These capacitors are modeled as a source that can provide only reactive power up to the capacitor's capacity. Details about the loads and the capacitor capacities are listed in Table IV. A cost function that minimizes the power losses in the network is used. The proposed approach was able to obtain a feasible solution that minimized the considered cost function. The injections from the capacitor along with the amount of of power drawn from the substation are summarized in Table II. The total power loss in the network in the solution is 37.52 KW. The voltage magnitudes at all the buses are depicted in Fig. 4, where it is clear that all the magnitudes lie within the prescribed limits.

For comparison purposes, it is worth emphasizing that the OpenDSS [21] software can provide flow solutions for the considered distribution networks without distributed energy sources, with maximum violation of the constraints in the order of 10^{-5}; in contrast, our algorithm is able to find feasible solutions even for cases where renewable energy sources are present, with accuracy in the order of 10^{-12}.

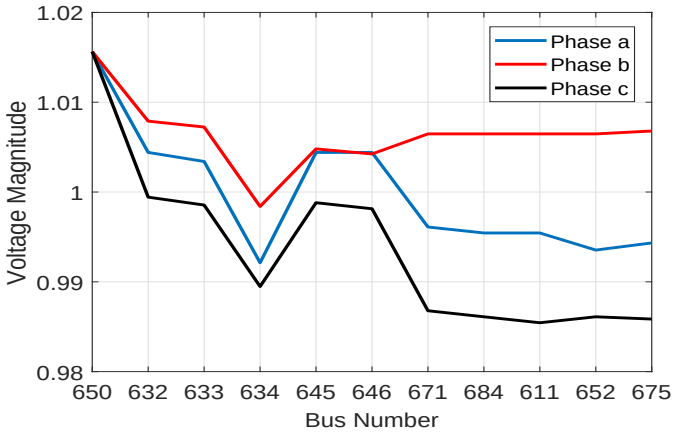

Fig. 4: The optimal voltage profile (in pu) using FPP-SCA for IEEE 13-node test feeder.

VI. Conclusions

The paper considered an AC OPF problem radial multiphase distribution networks with distributed energy sources. The QCQP problem formulation accounts for wye- and delta-connected generation units and loads and it was solved by leveraging the FPP-SCA methodology. The FPP-SCA was empirically shown to be very effective in solving the AC OPF when the power curtailed from RESs is to be minimized – a setup where competing solution methods based on convex relaxation approaches may fail in identifying even a feasible solution. To this end, two distribution feeders with both wye- and delta-connected units were utilized.

TABLE I: Results of the proposed approach [kVA].

Node	Power Injected		
	Phase a	**Phase b**	**Phase c**
799	701+482i	604.5+322.9i	577.85+201.44i
713	0	0	33+16.5i
718	33+16.4i	0	0
724	0	66+33i	0
729	66+32.9i	0	0
730	0	0	66+25i
732	0	0	66+33i
734	0	0	33+16.5i
737	66+33i	0	0
738	66+23i	0	0
741	0	0	33
740	0	0	66+0.5i
736	0	66+33i	0
735	0	0	108.9+19.66i

TABLE II: Results of the proposed approach in IEEE-13 feeder [kVA].

Node	Power Injected		
	Phase a	**Phase b**	**Phase c**
650	1228.4+584.15i	967.9+555.5i	1307.4+571.4i
611	0	0	100i
675	200i	0.8i	200i

Appendix
Construction of the Quadratic Matrices

The quadratic equality constraints (6) and (7) involve complex voltages $\mathbf{x}_v$, and currents $\mathbf{x}_i$ and $\mathbf{x}_\Delta$. As mentioned in Section III-B, the complex voltage $\tilde{\mathbf{x}}$ is constructed by concatenating the three vectors. In order to write the constraints (6) and (7) in the general form quadratic constraint $\tilde{\mathbf{x}}$, we need to construct quadratic matrices that represent the constraints. To this end, sort the lines in the network according the index of the receiving end of each line by a nondecreasing order. Note that, due to the tree structure assumed on the network, each bus except the substation appears only once as a receiving end. Let us define some transformation matrices as follows.

$$\begin{aligned}
\mathbf{T}_{v_k} &= [\mathbf{0}_{3\times 3k} \quad \mathbf{I}_{3\times 3} \quad \mathbf{0}_{3\times 3(n-k)} \quad \mathbf{0}_{3\times 3(n+1)} \quad \mathbf{0}_{3\times 3n}]^T \\
\mathbf{T}_{\Delta,k} &= [\mathbf{0}_{3\times 3(n+1)} \quad \mathbf{0}_{3\times 3k} \quad \mathbf{I}_{3\times 3} \quad \mathbf{0}_{3\times 3(n-k)} \quad \mathbf{0}_{3\times 3n}]^T \\
\mathbf{T}_{i_{kj}} &= [\mathbf{0}_{3\times 6(n+1)} \quad \mathbf{0}_{3\times 3(j-1)} \quad \mathbf{I}_{3\times 3} \quad \mathbf{0}_{3\times 3(n-j)}]^T \\
\mathbf{U}_{\Delta,k} &= [\mathbf{T}_{v_k} \quad \mathbf{T}_{\Delta_k}] \\
\mathbf{U}_{kj} &= [\mathbf{T}_{v_k} \quad \mathbf{T}_{i_{kj}}]
\end{aligned}$$

Hence, the vectors $\mathbf{x}_{\Delta,k}$ and $\mathbf{x}_{ki}$ are given by $\mathbf{U}_{\Delta,k}^T\tilde{\mathbf{x}}$ and $\mathbf{U}_{kj}^T\tilde{\mathbf{x}}$, respectively. Accordingly, the equality (6) can be re-written as

$$\begin{bmatrix} s_{\Delta,k}^{ab} \\ s_{\Delta,k}^{bc} \\ s_{\Delta,k}^{ca} \end{bmatrix} = \begin{bmatrix} \tilde{\mathbf{x}}^H\mathbf{U}_{\Delta,k}\left(E_{41}-E_{42}\right)\mathbf{U}_{\Delta,k}^T\tilde{\mathbf{x}} \\ \tilde{\mathbf{x}}^H\mathbf{U}_{\Delta,k}\left(E_{52}-E_{53}\right)\mathbf{U}_{\Delta,k}^T\tilde{\mathbf{x}} \\ \tilde{\mathbf{x}}^H\mathbf{U}_{\Delta,k}\left(E_{63}-E_{61}\right)\mathbf{U}_{\Delta,k}^T\tilde{\mathbf{x}} \end{bmatrix}, \quad \forall k \in \mathcal{N}. \tag{20}$$

These three complex equalities can be written as six real quadratic equations involving the complex vector $\tilde{\mathbf{x}}$. Introduce the Hermitian matrices $\mathbf{Y}_{\Delta,k}^{\phi}$ for all $\phi \in \Phi_\Delta$ which are as follows.

$$\begin{aligned}
\mathbf{Y}_{\Delta,k}^{ab} &= \frac{1}{2}\mathbf{U}_{\Delta,k}((E_{41}-E_{42})+(E_{41}-E_{42})^T)\mathbf{U}_{\Delta,k}^T \\
\tilde{\mathbf{Y}}_{\Delta,k}^{ab} &= \frac{1}{2i}\mathbf{U}_{\Delta,k}((E_{41}-E_{42})-(E_{41}-E_{42})^T)\mathbf{U}_{\Delta,k}^T \\
\mathbf{Y}_{\Delta,k}^{bc} &= \frac{1}{2}\mathbf{U}_{\Delta,k}((E_{52}-E_{53})+(E_{52}-E_{53})^T)\mathbf{U}_{\Delta,k}^T \\
\tilde{\mathbf{Y}}_{\Delta,k}^{bc} &= \frac{1}{2i}\mathbf{U}_{\Delta,k}((E_{52}-E_{53})-(E_{52}-E_{53})^T)\mathbf{U}_{\Delta,k}^T \\
\mathbf{Y}_{\Delta,k}^{ca} &= \frac{1}{2}\mathbf{U}_{\Delta,k}((E_{63}-E_{61})+(E_{63}-E_{61})^T)\mathbf{U}_{\Delta,k}^T \\
\tilde{\mathbf{Y}}_{\Delta,k}^{ca} &= \frac{1}{2i}\mathbf{U}_{\Delta,k}((E_{63}-E_{61})-(E_{63}-E_{61})^T)\mathbf{U}_{\Delta,k}^T
\end{aligned}$$

Then, the symmetric matrix $\mathbf{B}_{\Delta,k}^{\phi}$ for $\phi \in \Phi_\Delta$ can defined as

$$\mathbf{B}_{\Delta,k}^{\phi} = \begin{bmatrix} \Re\{\mathbf{Y}_{\Delta,k}^{\phi}\} & -\Im\{\mathbf{Y}_{\Delta,k}^{\phi}\} \\ \Im\{\mathbf{Y}_{\Delta,k}^{\phi}\} & \Re\{\mathbf{Y}_{\Delta,k}^{\phi}\} \end{bmatrix}. \tag{21}$$

Similarly, we construct $\tilde{\mathbf{B}}_{\text{Delta},k}^{\phi}$ as function $\tilde{\mathbf{Y}}_{\Delta,k}^{\phi}$. Using the matrices $\mathbf{U}_{kj}$ and $\mathbf{T}_{v_k}$, one can follow the same steps to construct the symmetric matrices $\mathbf{B}_{\text{Y},k}^{\phi}$ and $\tilde{\mathbf{B}}_{\text{Y},k}^{\phi}$ for all $k \in \mathcal{N}$ and $\phi \in \Phi$.

TABLE III: Load data for IEEE-37 distribution feeder [kVA].

Node	Loads						Available power from RES		
	Delta-connected			Wye-connected					
	ab	bc	ac	Phase a	Phase b	Phase c	Phase a	Phase b	Phase c
701	140+ 70i	140 + 70i	350 + 175i	0	0	0	0	0	0
702	0	0	0	0	0	0	0	0	0
705	0	0	0	0	0	0	0	0	0
712	0	0	85 + 40i	0	0	0	0	0	0
742	8 + 4i	85 + 40i	0	0	0	0	0	0	0
713	0	0	85 + 40i	0	0	0	0	0	33
704	0	0	0	0	0	0	0	0	0
714	17 + 8i	21+ 10i	0	0	0	0	0	0	0
718	85 + 40i	0	0	0	0	0	33	0	0
720	0	0	85 + 40i	0	0	0	0	0	0
707	0	0	0	0	0	0	0	0	0
724	0	42 + 21i	0	0	0	0	0	66	0
722	0	140 + 70i	21+ 10i	0	0	0	0	0	0
706	0	0	0	0	0	0	0	0	0
725	0	42 + 21i	0	0	0	0	0	0	0
703	0	0	0	0	0	0	0	0	0
727	0	0	42 + 21i	0	0	0	0	0	0
744	42 + 21i	0	0	0	0	0	0	0	0
729	42 + 21i	0	0	0	0	0	66	0	0
728	42 + 21i	42 + 21i	42 + 21i	65 + 30i	55 + 21i	42+ 21i	0	0	0
730	0	0	85 + 40i	0	0	0	0	0	66
709	0	0	0	0	0	0	0	0	0
731	0	85 + 40i	0	0	0	0	0	0	0
708	0	0	0	0	0	0	0	0	0
732	0	0	42 + 21i	0	0	0	0	0	66
733	85 + 40i	0	0	0	0	0	0	0	0
734	0	0	42 + 21i	0	0	0	0	0	33
737	140 + 70i	0	0	0	0	0	66	0	0
738	126 + 62i	0	0	0	0	0	66	0	0
711	0	0	0	0	0	0	0	0	0
741	0	0	42 + 21i	0	0	0	0	0	33
740	0	0	85 + 40i	0	0	0	0	0	66
710	0	0	0	0	0	0	0	0	0
736	0	42 + 21i	0	0	0	0	0	66	0
735	0	0	85 + 40i	0	0	0	0	0	115.44

TABLE IV: Load data for IEEE-13 distribution feeder [kVA].

Node	Loads						Available reactive power from Caps		
	Delta-connected			Wye-connected					
	ab	bc	ac	Phase a	Phase b	Phase c	Phase a	Phase b	Phase c
632	0	0	0	8.5+5i	33+19i	58.5+34i	0	0	0
633	0	0	0	0	0	0	0	0	0
634	0	0	0	160+110i	120+90i	120+90i	0	0	0
645	0	0	0	0	170+125i	0	0	0	0
646	0	230+132i	0	0	0	0	0	0	0
671	385+220i	385+220i	555+371i	8.5+5i	33+19i	58.5+34i	0	0	0
684	0	0	0	0	0	0	0	0	0
611	0	0	0	0	0	170+80i	0	0	100i
652	0	0	0	128+86i	0	0	0	0	0
675	0	0	0	485+190i	68+60i	290+212i	200i	200i	200i

REFERENCES

[1] J. Carpentier, "Optimal power flows," *International Journal of Electrical Power and Energy Systems*, vol. 1, no. 1, pp. 3 – 15, 1979.

[2] J. A. Taylor, S. V. Dhople, and D. S. Callaway, "Power systems without fuel," *Renewable & Sustainable Energy Reviews*, vol. 57, pp. 1322–1336, May 2016.

[3] J. Lavaei and S. Low, "Zero Duality Gap in Optimal Power Flow Problem," *IEEE Trans. on Power Systems*, vol. 27, no. 1, pp. 92–107, Feb 2012.

[4] E. Dall'Anese, S. V. Dhople, and G. B. Giannakis, "Optimal dispatch of photovoltaic inverters in residential distribution systems," *IEEE Trans. on Sustainable Energy*, vol. 5, no. 2, pp. 487–497, April 2014.

[5] A. H. Mohsenian-Rad, V. W. S. Wong, J. Jatskevich, R. Schober, and A. Leon-Garcia, "Autonomous demand-side management based on game-theoretic energy consumption scheduling for the future smart grid," *IEEE Trans. on Smart Grid*, vol. 1, no. 3, pp. 320–331, Dec. 2010.

[6] M. A. Ortega-Vazquez, F. Bouffard, and V. Silva, "Electric vehicle Aggregator/System operator coordination for charging scheduling and services procurement," *IEEE Transactions on Power Systems*, vol. 28, no. 2, pp. 1806–1815, May 2013.

[7] S. Paudyal, C. A. Canizares, and K. Bhattacharya, "Optimal operation of distribution feeders in smart grids," *IEEE Trans. on Ind. Electron.*, vol. 58, no. 10, pp. 4495–4503, Oct. 2011.

[8] M. Farivar, R. Neal, C. Clarke, and S. Low, "Optimal inverter VAR control in distribution systems with high PV penetration," in *IEEE PES General Meeting*, San Diego, CA, Jul. 2012.

[9] K. Turitsyn, P. Sulc, S. Backhaus, and M. Chertkov, "Options for control

of reactive power by distributed photovoltaic generators," *Proc. of the IEEE*, vol. 99, no. 6, pp. 1063–1073, 2011.

[10] K. Lehmann, A. Grastien, and P. V. Hentenryck, "AC-Feasibility on Tree Networks is NP-Hard," *IEEE Trans. on Power Systems*, vol. 31, no. 1, pp. 798–801, Jan 2016.

[11] O. Mehanna, K. Huang, B. Gopalakrishnan, A. Konar, and N. Sidiropoulos, "Feasible point pursuit and successive approximation of non-convex QCQPs," *IEEE Signal Processing Letters*, vol. 22, no. 7, pp. 804–808, July 2015.

[12] A. S. Zamzam, N. D. Sidiropoulos, and E. Dall'Anese, "Beyond relaxation and Newton-Raphson: Solving AC OPF for multi-phase systems with renewables," *IEEE Trans. Smart Grid*, vol. PP, no. 99, pp. 1–1, 2017.

[13] L. Gan, N. Li, U. Topcu, and S. H. Low, "Exact convex relaxation of optimal power flow in radial networks," *IEEE Trans. on Automatic Control*, vol. 60, no. 1, pp. 72–87, 2015.

[14] R. Jabr, "Radial distribution load flow using conic programming," *IEEE Trans. on Power Systems*, vol. 21, no. 3, pp. 1458–1459, Aug 2006.

[15] E. Dall'Anese, H. Zhu, and G. B. Giannakis, "Distributed optimal power flow for smart microgrids," *IEEE Trans. on Smart Grid*, vol. 4, no. 3, pp. 1464–1475, Sep 2013.

[16] J. Lavaei, D. Tse, and B. Zhang, "Geometry of power flows in tree networks," in *IEEE Power and Energy Society General Meeting*, San Diego,CA, July 2012.

[17] L. Gan and S. H. Low, "Convex relaxations and linear approximation for optimal power flow in multiphase radial networks," in *Power Systrem Computation Conference*, Wroclaw, Poland, August 2014.

[18] B. A. Robbins, H. Zhu, and A. D. Domínguez-Garca, "Optimal tap setting of voltage regulation transformers in unbalanced distribution systems," *IEEE Trans. on Power Systems*, vol. 31, no. 1, pp. 256–267, Jan 2016.

[19] D. Molzahn and I. Hiskens, "Moment-based relaxation of the optimal power flow problem," in *Power Systems Computation Conference*, Wrocaw, Poland, Aug 2014.

[20] D. K. Molzahn, C. Josz, I. A. Hiskens, and P. Panciatici, "A Laplacian-Based Approach for Finding Near Globally Optimal Solutions to OPF Problems," *IEEE Transactions on Power Systems*, vol. 32, no. 1, pp. 305–315, Jan 2017.

[21] R. C. Dugan, "Reference guide: The open distribution system simulator (OpenDSS)," *Electric Power Research Institute, Inc*, vol. 7, 2012.